The Calphad Method

or

the Virtual Thermochemistry Lab

Bengt Hallstedt

Nichtmetallische Werkstoffe
ETH Zürich

Outline

- Phase diagrams
- Thermodynamics $\rightarrow$ phase diagrams
- The Calphad method
- Virtues of Calphad
- Summary

Phase Diagram of Water (H_2O)

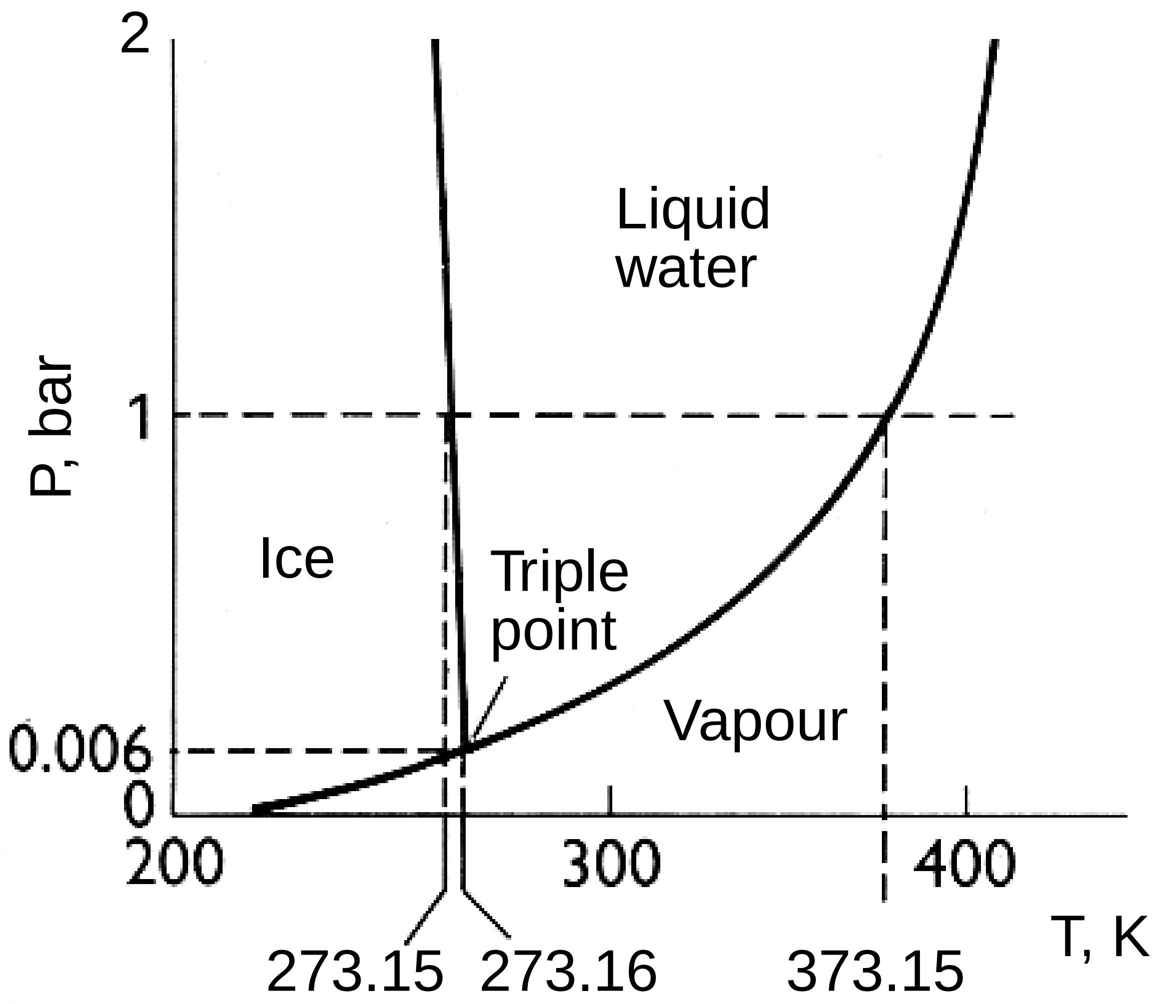

Water–Salt Phase Diagram

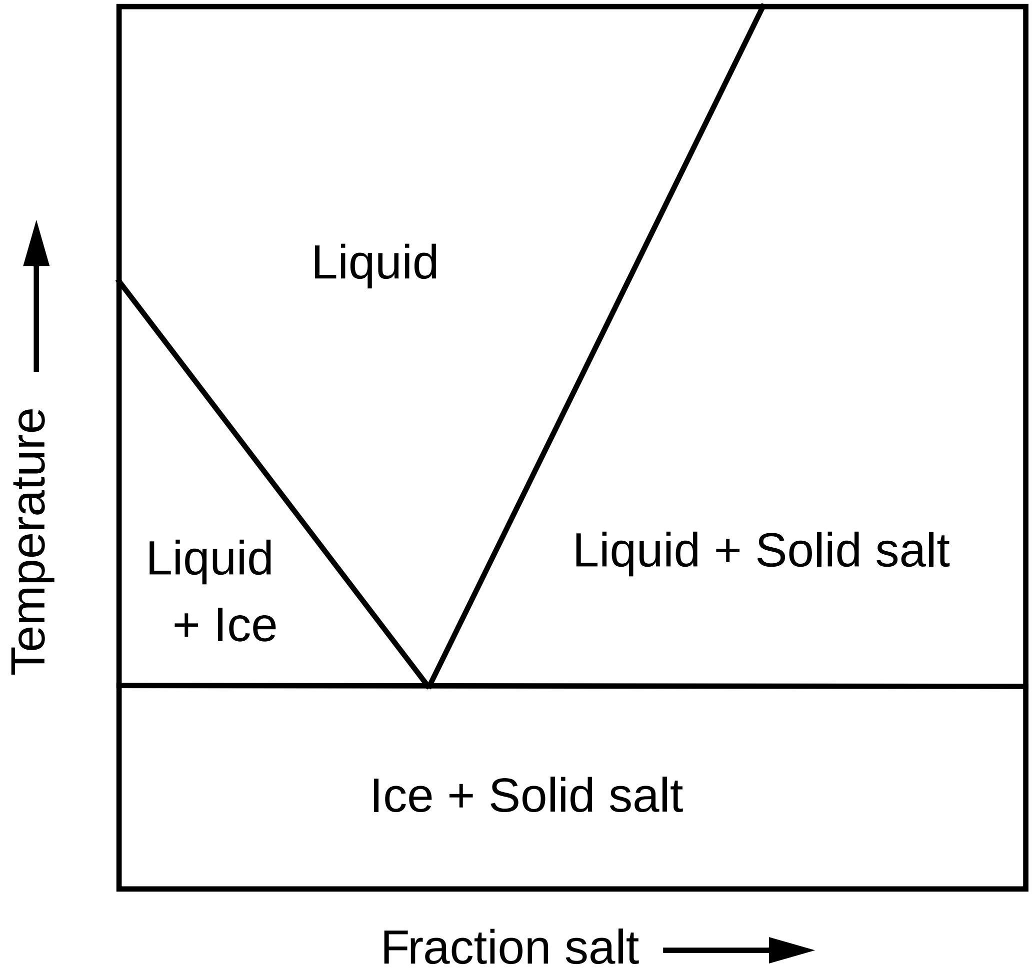

Thermodynamics → Phase Diagrams

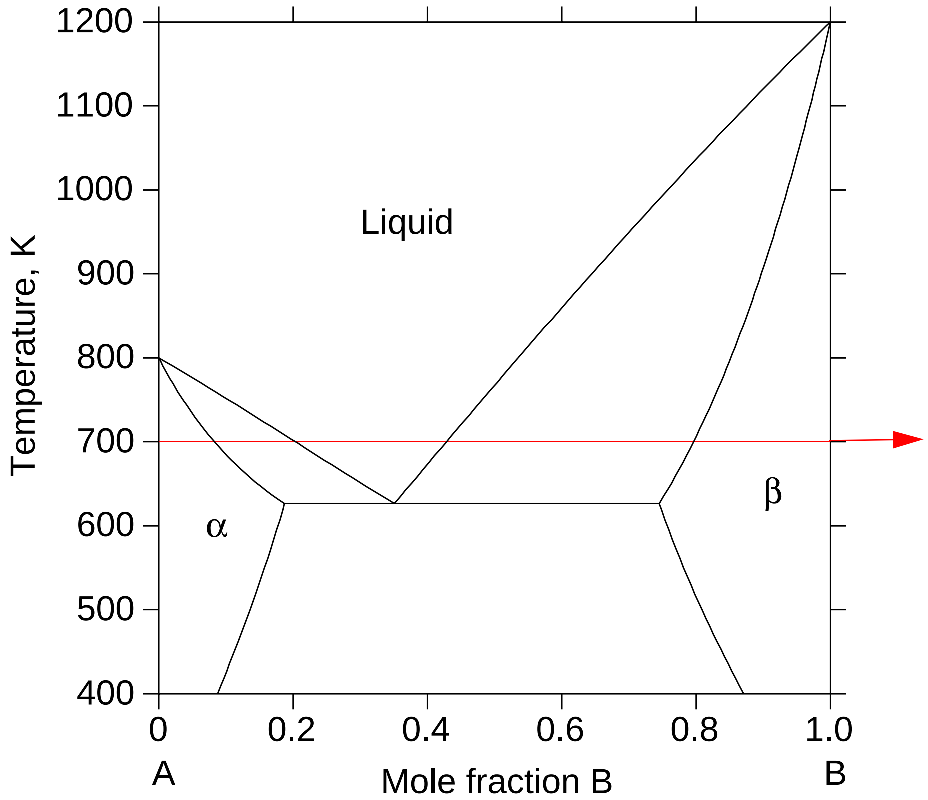

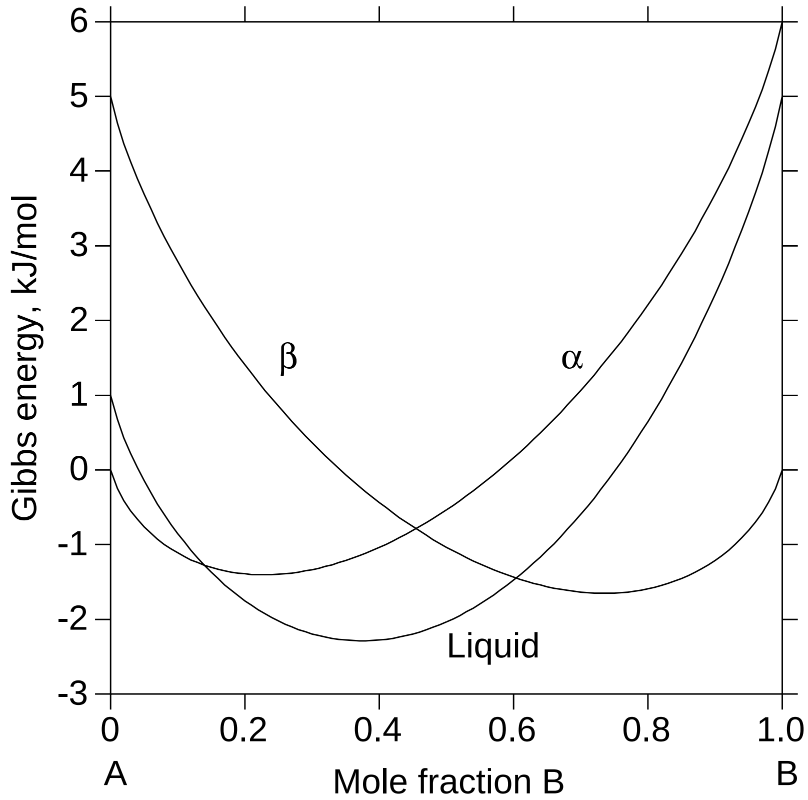

$$G_m = x_A {}^\circ G_A + x_B {}^\circ G_B + RT(x_A \ln x_A + x_B \ln x_B) + x_A x_B L$$

The Calphad Method

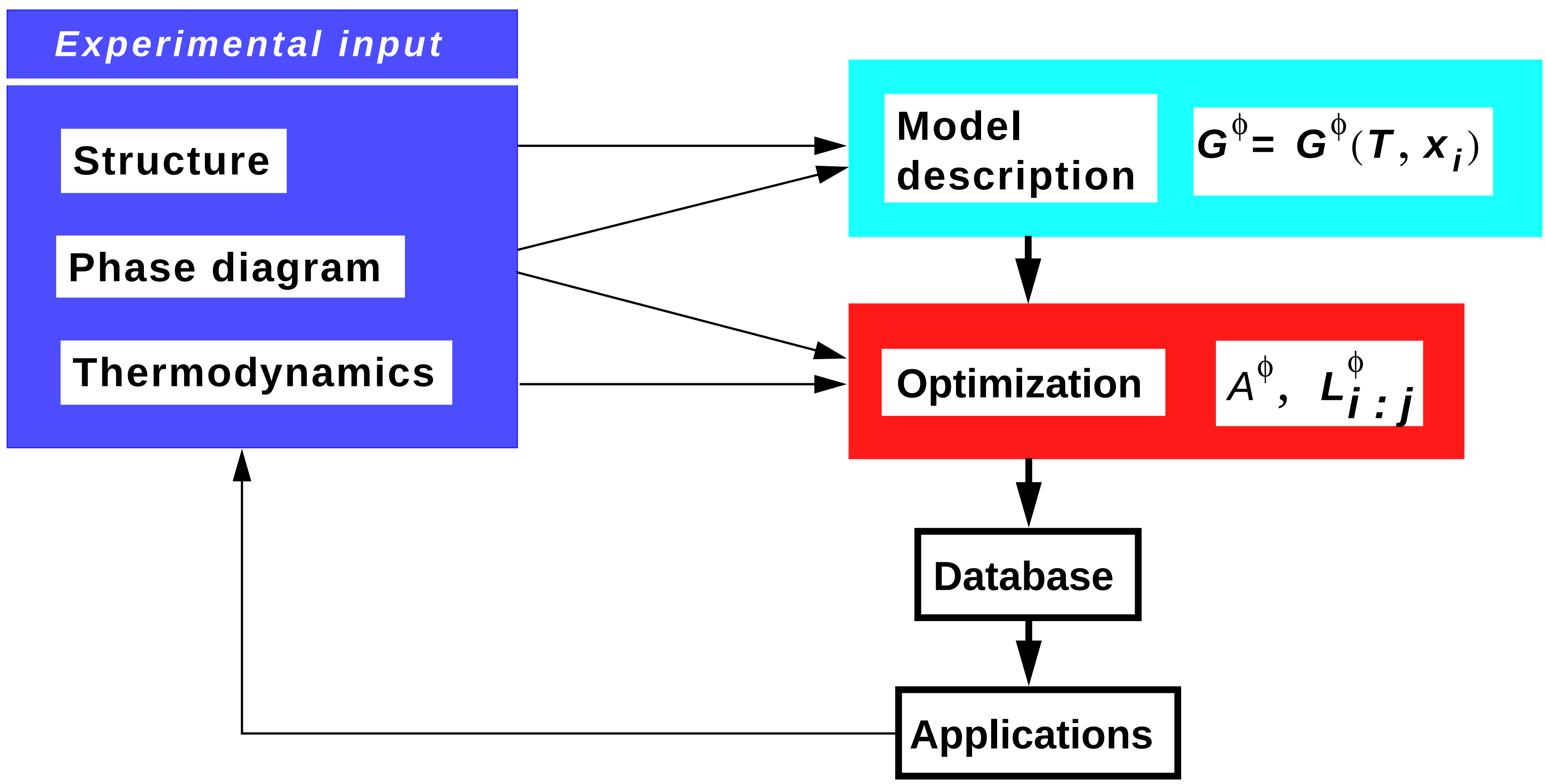

Experimental Data

Structure	Phase diagram	Thermochemical data
(ideal composition)	Composition Melting temperature or max / min temperature	Enthalpy of formation (ΔH_f) Entropy (S_{298}, from C_P) Heat capacity (C_P) Heat content ($H - H_{298}$) Gibbs energy of formation (from emf or partial pressure)
Sublattice occupation (Defects)	max / min solubility as f(T)	Chemical potential as f(T,x) Enthalpy of mixing

ETH Materials

The Five Virtues

- Consistency
- Multicomponent systems
- Metastable states
- Phase transformation
- Model calculations

Defect Chemistry of $La_{1-y}MnO_{3\pm\delta}$

Sublattice model:

$(La^{3+},Va)_1(Mn^{3+},Mn^{2+},Mn^{4+},Va)_1(O^{2-},Va)_3$

Possible charge compensation when $y \neq 0$:

1. Formation of oxygen vacancies

2. Oxidation of Mn^{+3} to Mn^{+4}

Oxygen Nonstoichiometry of $La_{1-y}MnO_{3\pm\delta}$

Formation of oxygen vacancies

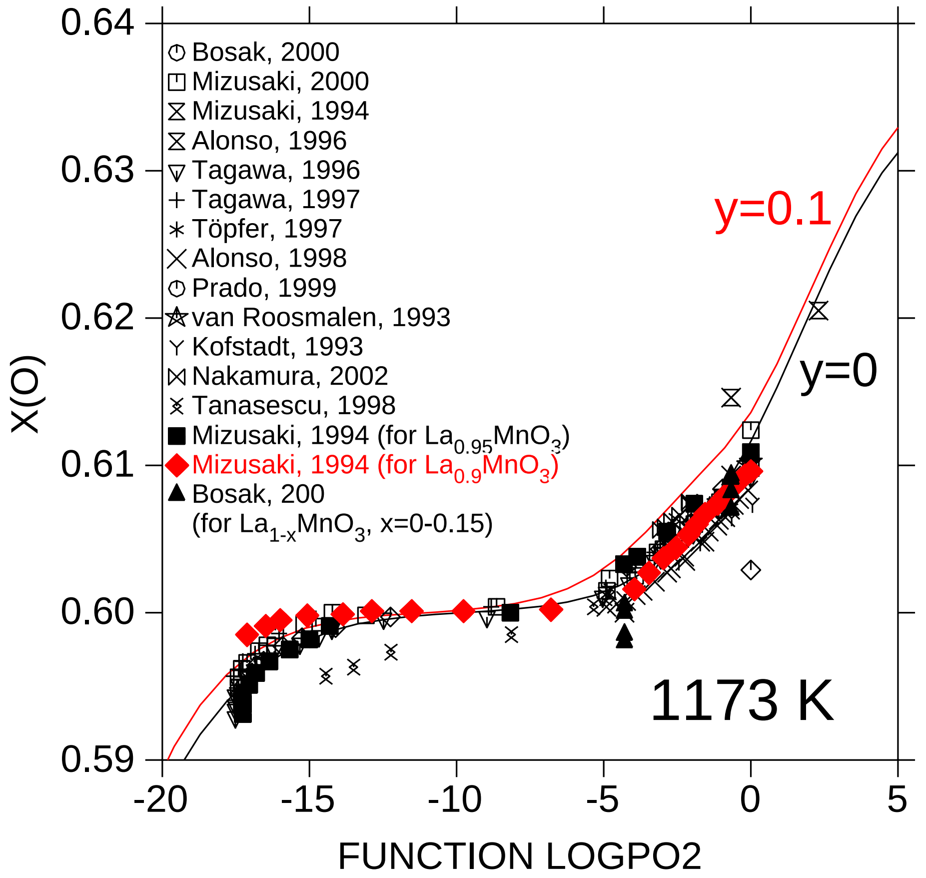

Oxidation of Mn^{+3} to Mn^{+4}

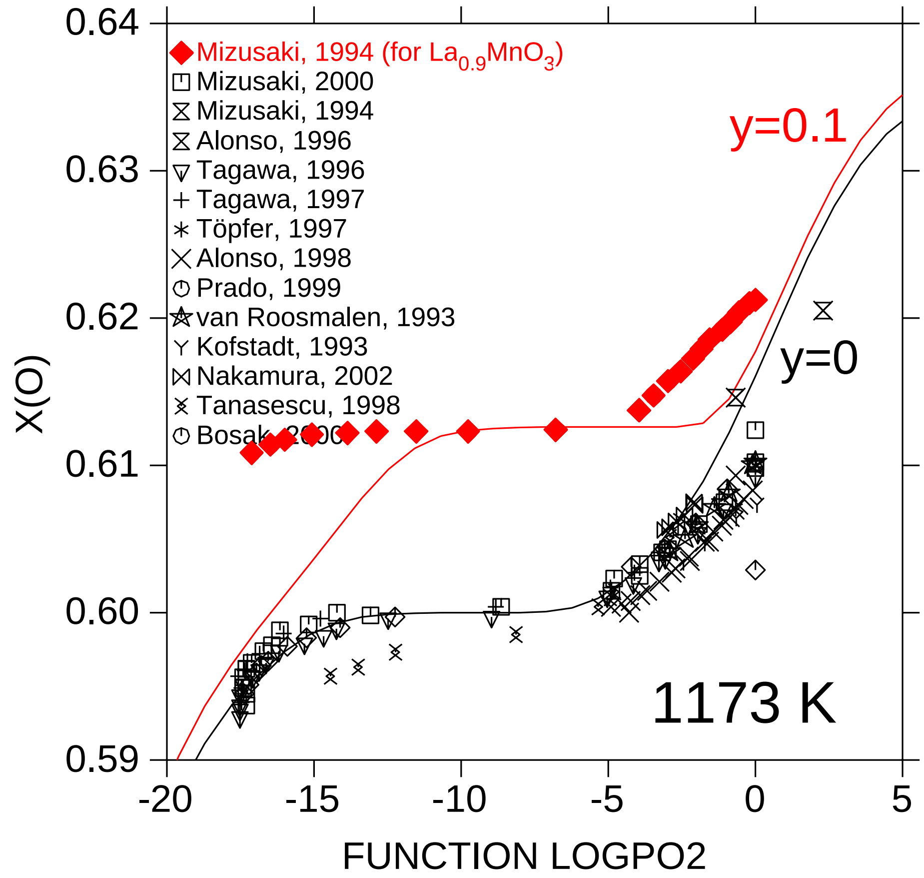

N. Grundy et al., current work, 2002–03

ETH Materials

Oxygen Nonstoichiometry of $La_{1-y}MnO_{3\pm\delta}$

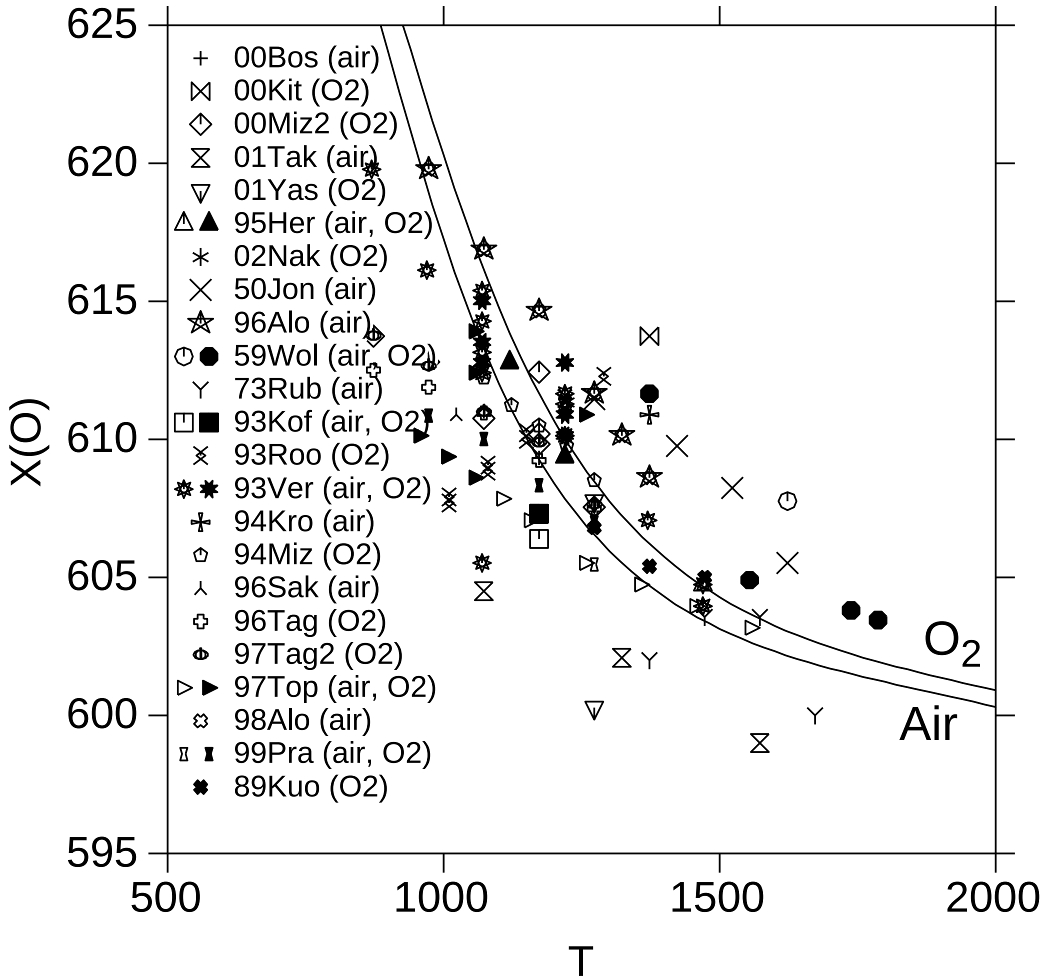

N. Grundy et al., current work, 2002–03

ETH Materials

Microstructure of $Bi_2Sr_2CaCu_2O_{8+\delta}$ (Bi-2212) Thick Film on Ag

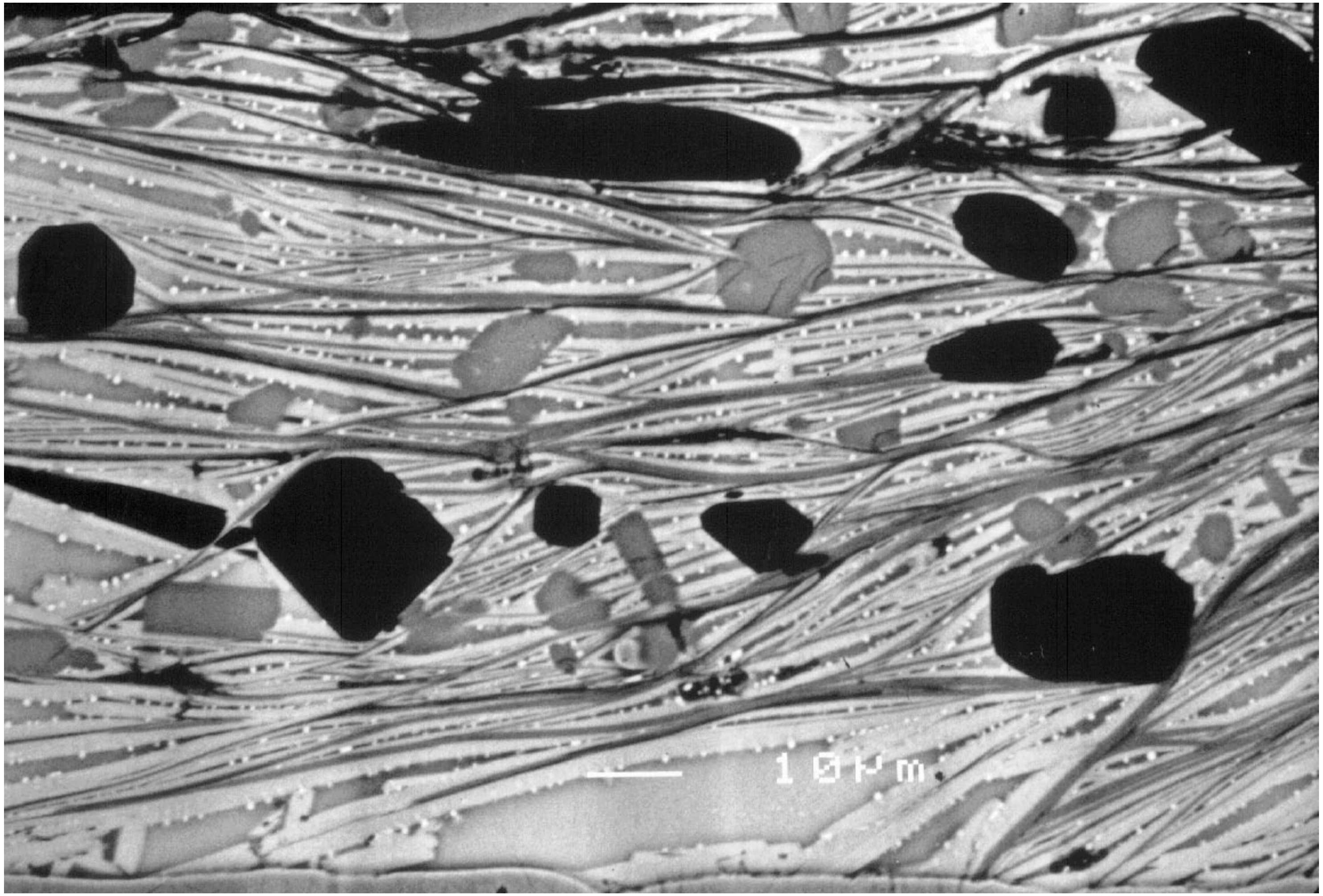

0<u>14</u>x<u>24</u>

9<u>11</u>50

Bi-2212
silver

liquid
“bright cloud”

Ag substrate

from Th. Lang, 1996

T_{max}=1177 K, T_{quench}=1143 K (in O_2)

ETH Materials

Bi–Sr–Ca–Cu–O Experimental Section at n_{Cu} = 2, 830°C

R. Müller et al., *Physica C*, **203**, 299–314 (1992)

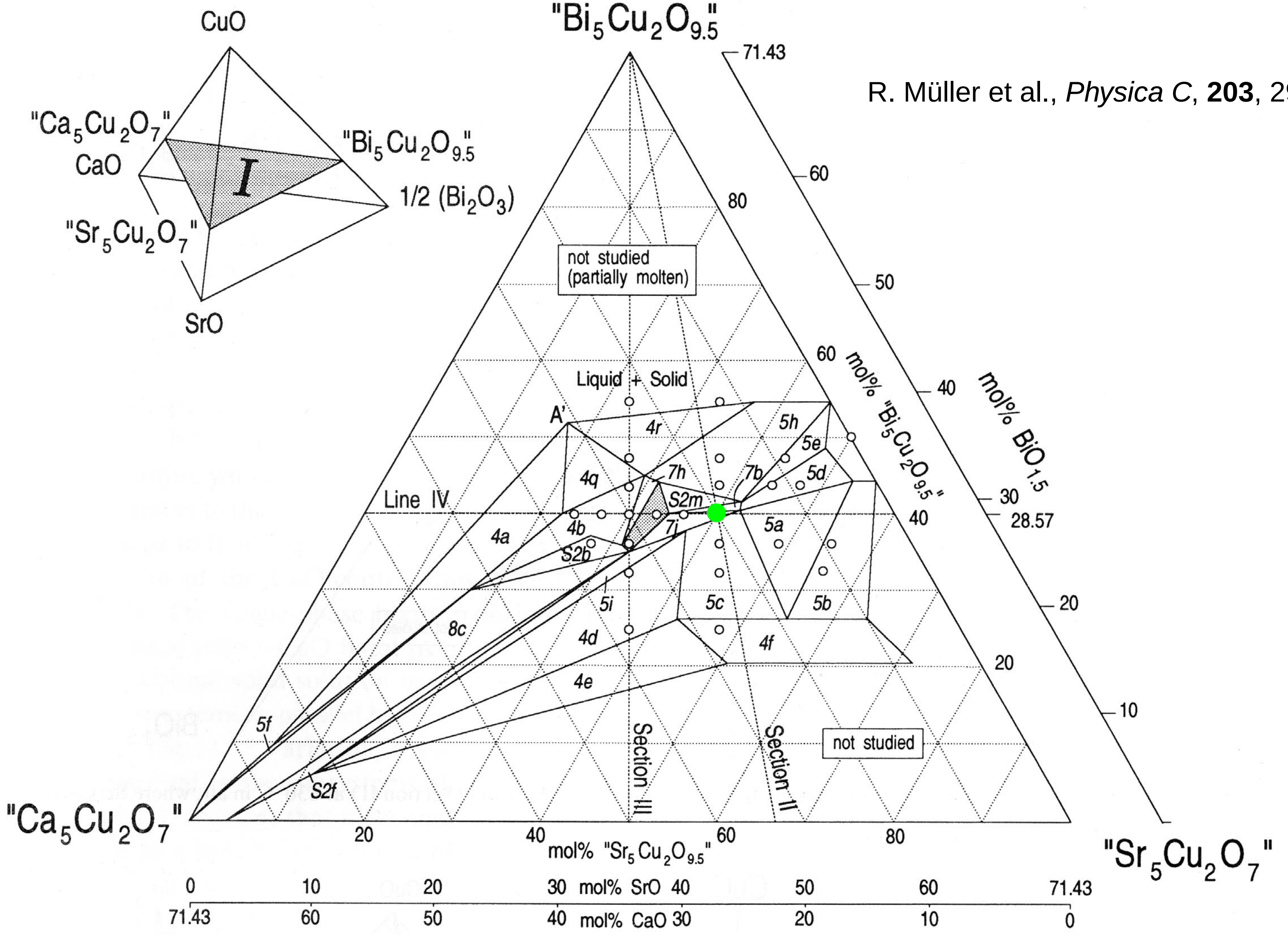

Modelling the $Bi_2Sr_2CaCu_2O_{8+\delta}$ Phase

Structure

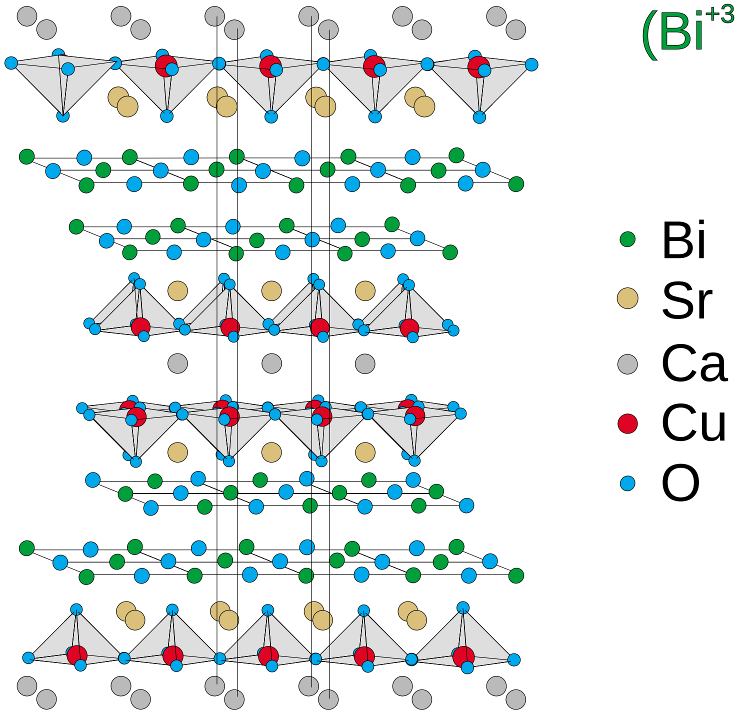

Sublattice Model

$(Bi^{+3},Bi^{+5})_2(Sr^{+2},Ca^{+2},Bi^{+3})_2(Ca^{+2})(Cu^{+2},Cu^{+3})_2(O^{-2})_8(Va,O^{-2})_x$

Gibbs Energy

$$G^{2212} = \Sigma\, {}^{o}G_i - T\, S^{ideal} + \Sigma\, y_j\, y_k\, L_{jk}$$

Parameters

${}^{o}G_{2212}$	$\Delta G(Sr^{+2} - Bi^{+3})$	$\Delta G(Bi^{+3} - Bi^{+5})$
	$\Delta G(Sr^{+2} - Ca^{+2})$	$\Delta G(Cu^{+2} - Cu^{+3})$

Solid Solution Region of Bi-2212

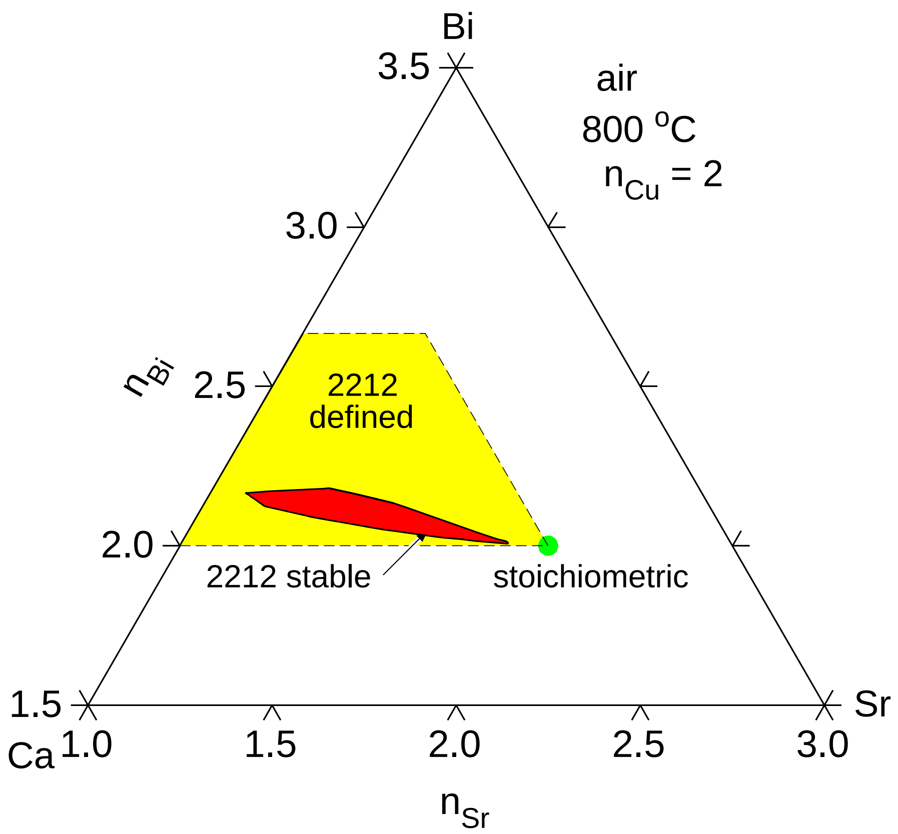

Present model

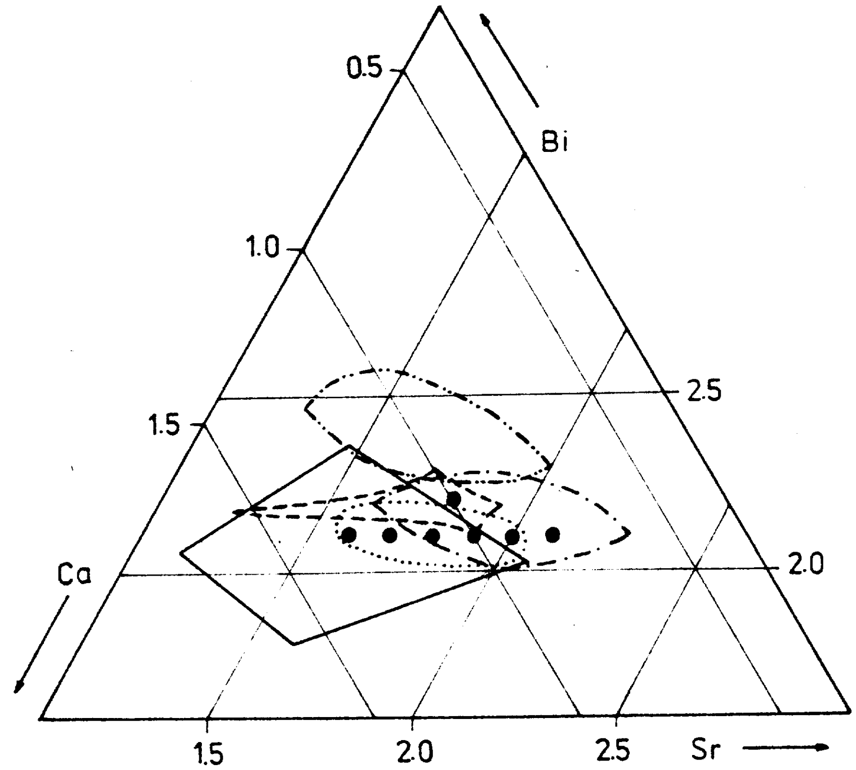

Experimental results, different sources

K. Knízek *et al.*, *Physica C*, **216**, 211–18 (1993)

Calculated Isothermal Section at n_{Cu} = 2, 800°C

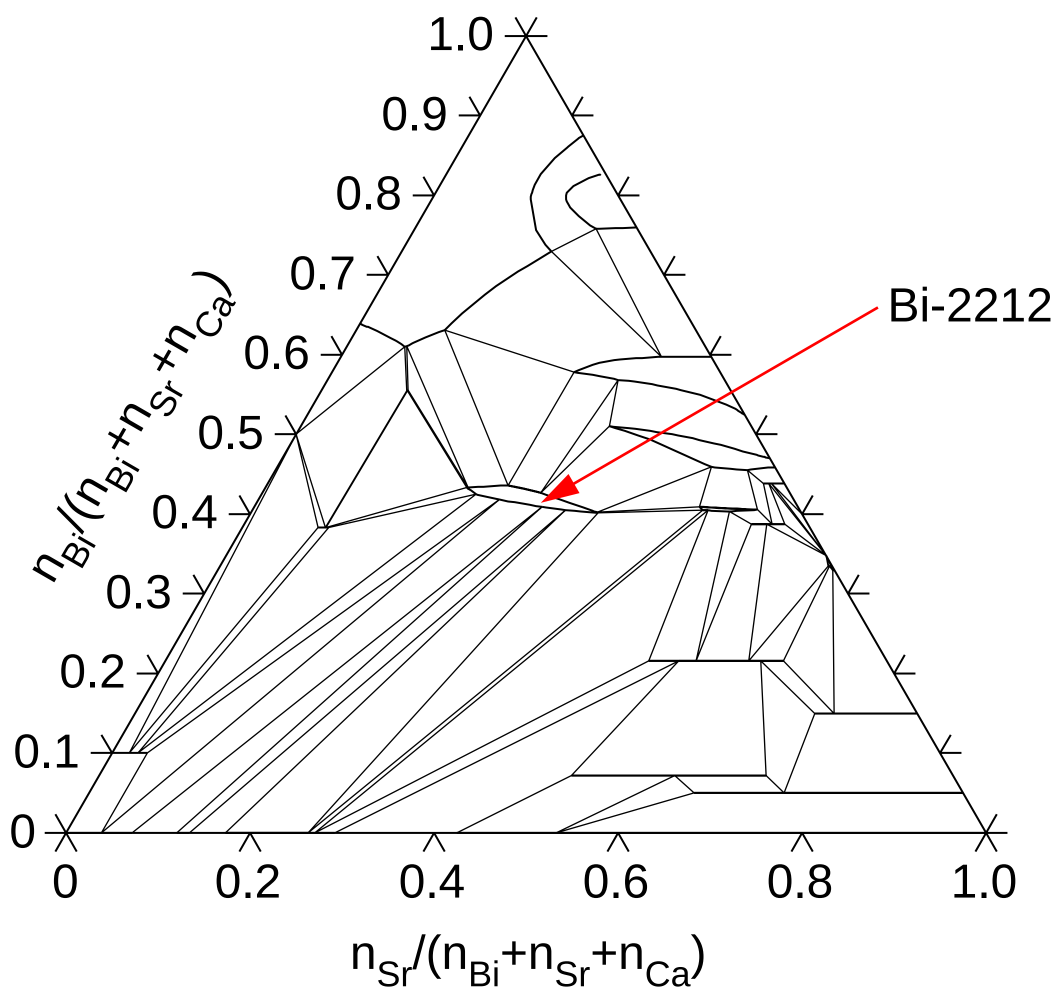

B. Hallstedt, et al., unpublished work, 1997

The Fe–C Phase Diagram

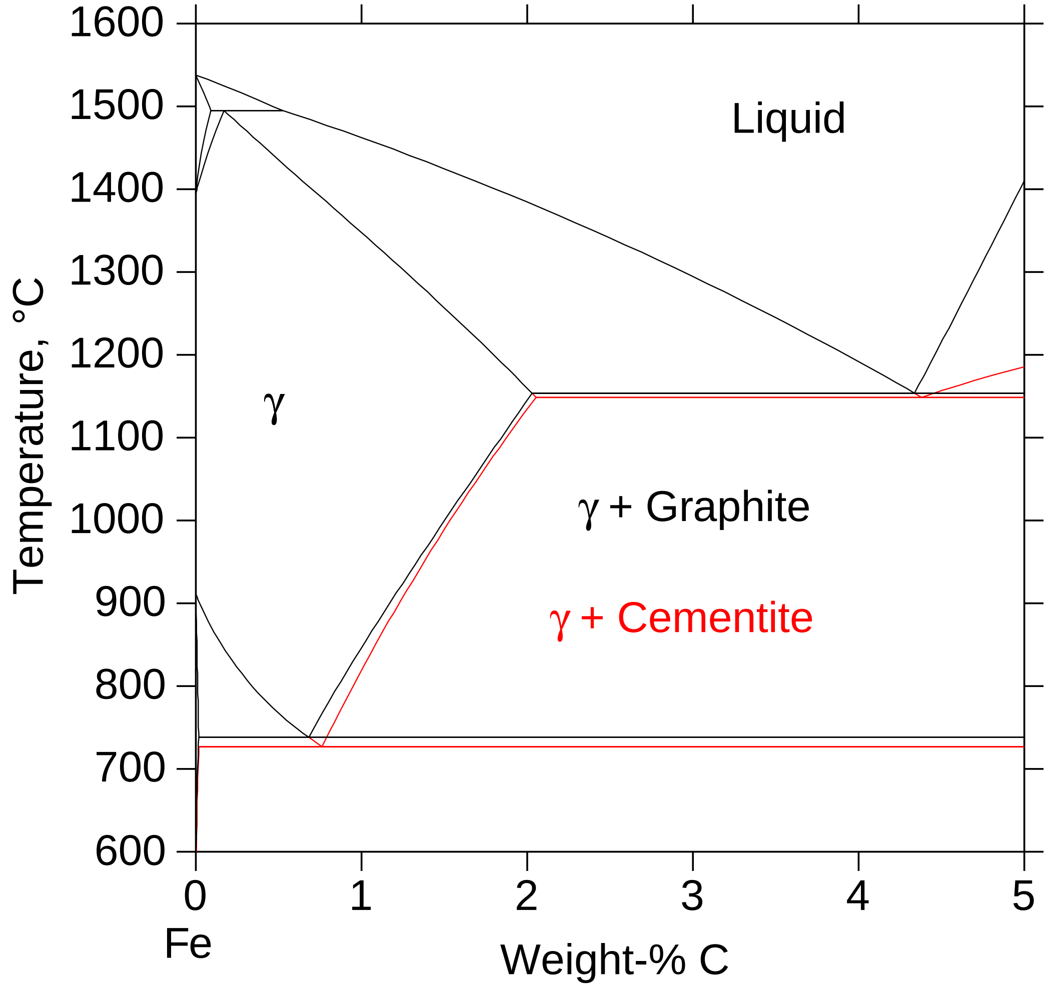

Ni–Cr Phase Diagram

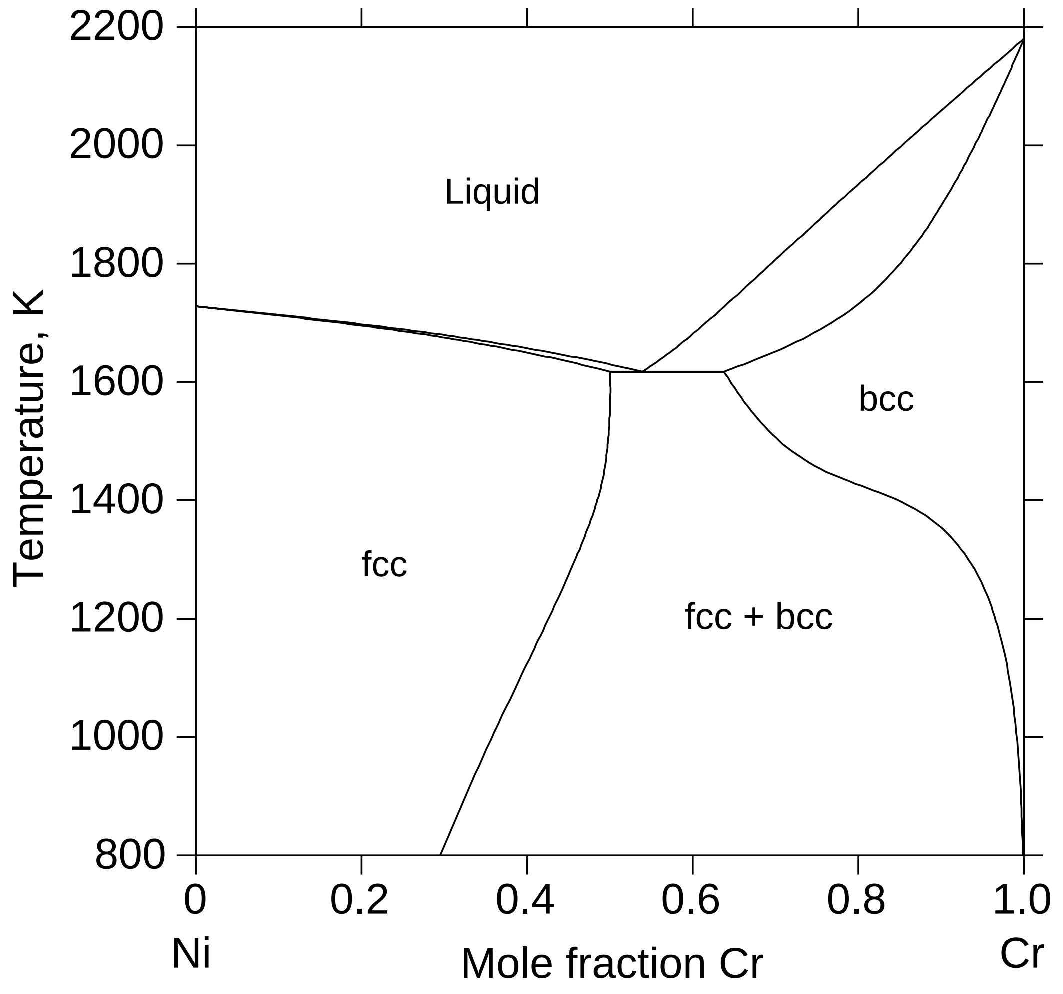

Ni–Cr Including Metastable Extensions

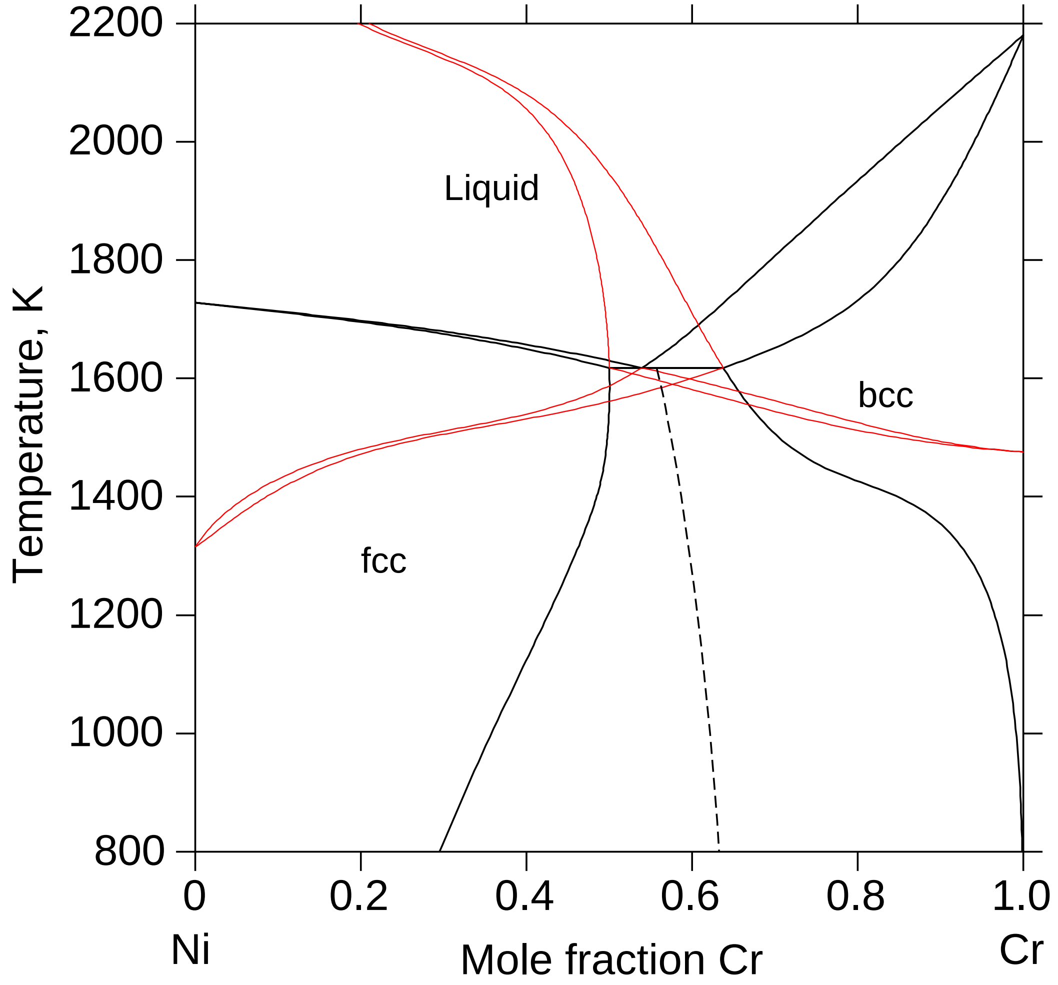

Diffusion in the B2 Phase in Al–Fe–Ni

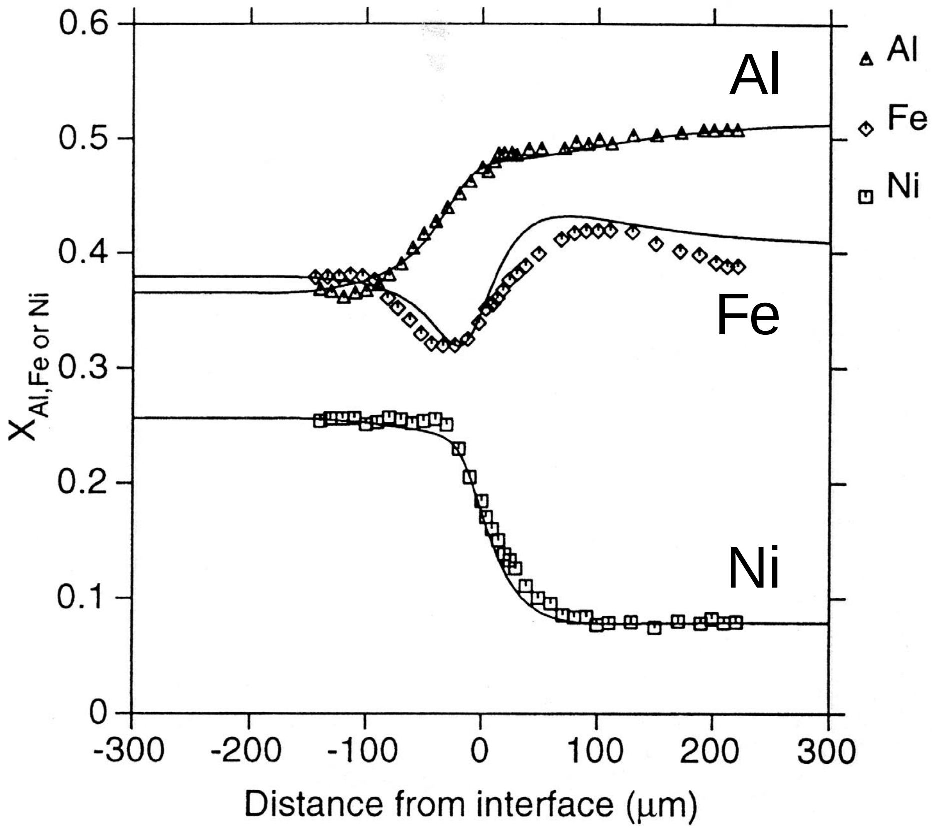

Diffusion couple heated 96 h at 1277 K

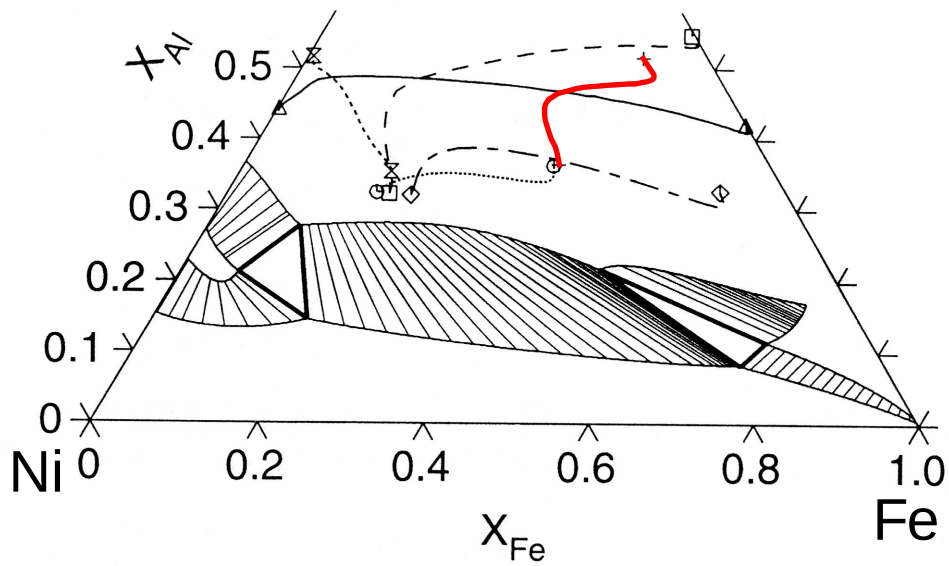

From T. Helander and J. Ågren, *Acta Mater.*, **47**, 3291–3300 (1999)

Simple Model Systems

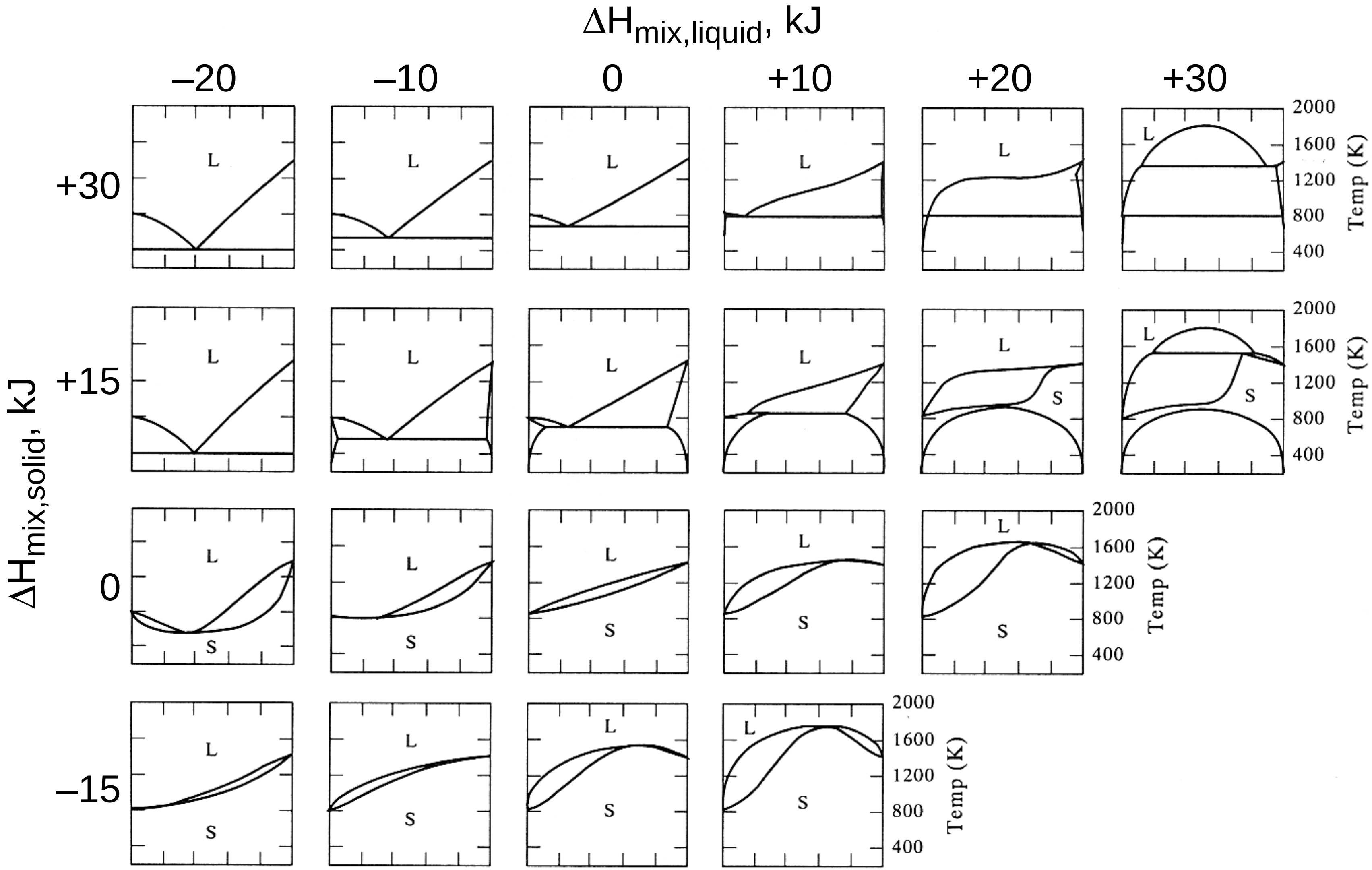

Summary

The five advantages

- Thermodynamic consistency
- Multicomponent systems
- Metastable states
- Phase transformations
- Understanding thermochemistry / teaching

Thanks to...

Prof. Ludwig J. Gauckler

Daniel Risold
Jérôme Assal
Nicholas Grundy
Ming Chen